

NASA TECHNICAL NOTE



NASA TN D-4957

C.1

NASA TN D-4957



LOAN COPY: RETURN TO
AFWL (WLIL-2)
KIRTLAND AFB, N MEX

**INVISCID FLOW ANALYSIS OF
TWO PARALLEL SLOT JETS
IMPINGING NORMALLY ON A SURFACE**

by Richard T. Gedney and Robert Siegel

*Lewis Research Center
Cleveland, Ohio*



INVISCID FLOW ANALYSIS OF TWO PARALLEL SLOT JETS
IMPINGING NORMALLY ON A SURFACE

By Richard T. Gedney and Robert Siegel

Lewis Research Center
Cleveland, Ohio

NATIONAL AERONAUTICS AND SPACE ADMINISTRATION

For sale by the Clearinghouse for Federal Scientific and Technical Information
Springfield, Virginia 22151 - CFSTI price \$3.00

ABSTRACT

Conformal mapping was applied to obtain the flow pattern for two parallel jets of finite width originating from infinity and impinging normally on a plate. The ratio of the half spacing between the jets to the jet width (S/H) is the single parameter governing the flow. Analytical expressions and graphs are given for the free streamlines, internal streamlines, and pressure coefficient along the plate for various values of the S/H ratio. A portion of each jet flows outward along the plate and the remaining flow is a recirculation back toward infinity along the axis between the jets. The amount of recirculation is given as a function of the S/H ratio.

INVISCID FLOW ANALYSIS OF TWO PARALLEL SLOT JETS IMPINGING NORMALLY ON A SURFACE

by Richard T. Gedney and Robert Siegel

Lewis Research Center

SUMMARY

Conformal mapping was applied to obtain the flow pattern for two parallel inviscid jets of finite width originating from infinity and impinging normally on a plate. The boundaries of the flow consist of the plate and free streamlines separating the jets and the fluid surrounding them. The mapping procedure yields a solution of Laplace's equation for the stream and potential functions in the jet flow region. The position of the free streamlines bounding the flow as well as the internal streamlines are uniquely determined by the mapping procedure.

The ratio of the half spacing between the jets to the jet width (S/H) is the single parameter governing the flow. Analytical expressions and graphs are given for the free streamlines, internal streamlines, and pressure coefficient along the plate for various values of S/H . A portion of each jet flows outward along the plate and the remaining flow is a recirculation back toward infinity along the axis between the jets. The amount of recirculation is given as a function of S/H .

The solution provides the potential flow distribution that is required to compute the boundary layer and heat transfer along the plate. Such computations are of interest in laminar impingement cooling or heating applications.

INTRODUCTION

Several industrial operations employ single and multiple jets of a variety of cross sections impinging on surfaces for cooling and heating purposes. The annealing of sheet metal, the tempering of glass and the drying of paper are some of the important applications. In addition, ground effect machines and vertical take-off aircraft utilize impinging jets. Because of these many applications, the understanding of jet impingement features is important. The current analysis considers the effects of two plane parallel jets of

equal width impinging on a flat surface. These slot jets are considered to originate at an infinite distance from the surface and be perpendicular to it.

The classical inviscid incompressible solution for flow originating from a single slot jet at infinity and impinging on a flat surface is given in reference 1. This solution shows that the velocity of the incoming jet is constant until approximately two jet widths away from the surface. Therefore, we can expect that the solution with the flow originating from infinity would yield essentially the same results as for a jet originating at uniform velocity from a nozzle at a finite distance larger than two jet widths away from the surface.

Experimental pressure distributions along the surface for a single slot jet when the jet and surrounding fluid are both air are reported in reference 2. The reference 1 theory is found to be in good agreement with experimental results provided the ratio of the nozzle distance from the surface, to the jet width is 2 to 4 and the jet Reynolds number is small enough (of order $Re \leq 5500$). (No pressure data above 5500 was published in ref. 2.) When the jet is too far from the plate, entrainment of the surrounding fluid becomes significant. When the jet nozzle is too close to the plate, the jet exit velocity becomes nonuniform as it is affected by the pressure buildup of the fluid striking the plate. When the jet Reynolds number is too high, the fluid may be highly turbulent at the nozzle exit. The experimental results thus indicate that if one is careful to keep the cited restrictions in mind, limited information for the impingement region can be obtained by the study of inviscid jets flowing from infinity.

Little theoretical work has been done for the case of multiple impinging jets and this is the reason for the study of the two slot jet configuration considered herein. The shape of the free streamline boundaries, the internal flow streamlines, the amount of flow that is recirculated, and the surface pressure distributions are found. Results are presented for various ratios of the half spacings between the jets to the jet width (S/H).

SYMBOLS

A	dimensionless distance in t plane between points 7 and 8
a	point of maximum velocity along wall, fig. 2
B, C, D, E	coefficients defined in eqs. (12) and (14)
b	point where $v = 0$ on free streamline, fig. 2
C_p	pressure coefficient, $(p - p_a) / (1/2\rho_j V_\infty^2)$
g	gravitational acceleration
H	width of undisturbed jet, fig. 1

h_{1-9} , h_{2-4} , h_{5-6}	} dimensionless jet widths, fig. 2
K	a constant
p	pressure
Re	jet Reynolds number, $V_\infty H \rho_j / \mu_j$
S	half spacing between two incident jets
s	dimensionless half spacing, S/H
T	complex variable in T plane, fig. 6
t	complex variable in auxiliary t plane, $t = \xi + i\eta$, fig. 4
U	velocity in X direction
u	dimensionless velocity in x direction, $U/ V_\infty $
V	velocity in Y direction
$ V_\infty $	speed of incoming jet at infinity
v	dimensionless velocity in y direction, $V/ V_\infty $
W	dimensionless complex potential, $\Phi + i\psi$
X, Y	rectangular coordinates
x, y	dimensionless coordinates, X/H , Y/H
z	complex variable, $x + iy$
α	angle between the conjugate velocity vector and the real axis
β	argument in the t plane
ζ	dimensionless complex conjugate vector velocity, $u - iv$
η	imaginary part of t
μ	absolute viscosity
ξ	real part of t
ρ	density
Φ	dimensionless velocity potential function
ψ	dimensionless stream function

Subscripts:

a	atmosphere outside jet	
j	jet	
0	refers to the origin	
1, 2, 3, } 4, 5, 6, } 7, 8, 9 }	these numbers refer to the points so labeled in fig. 2	
∞		infinity

ANALYSIS

Configuration

The slot jet configuration that was analyzed is shown in figure 1. It consists of two parallel jets each of the same width H and spaced $2S$ apart. The jets originate at $Y = +\infty$ and flow downward until they impinge on the horizontal plane at $Y = 0$. The jet velocities at infinity are uniform across the jet width and have the magnitude $|V_\infty|$. The plane at $Y = 0$ is normal to the jet axes. As the jets impinge on the flat plate the flow from each jet divides into two parts. One part of each jet flows outward along the plate to infinity. The other parts of each jet impact each other, forming a vertical column moving upward along the positive Y axis. Since the jets are of equal width and velocity, the flow is symmetric about the Y axis. Therefore, the configuration will be analyzed by considering the flow in the first quadrant of the X - Y plane.

Assumptions

It is important to be aware of the basic assumptions employed in this jet analysis. The flow is considered steady, inviscid, irrotational, and incompressible. The fluid surrounding the jets is stationary and of constant pressure. Further, the boundary between the jets and the surrounding fluid is considered a slipline so there is no entrainment of surrounding fluid into the jet. As a result, the slipline is also a streamline. This slipline boundary will hereafter be referred to as the free streamline. The assumption that the pressure along the free streamline is constant requires not only stationary surrounding fluid but also neglect of gravity effects. The neglect of gravity in the jet flow solution is equivalent to saying that the jet Froude number V_∞^2/gH , which is the ratio of inertia forces to body forces, is large.

Complex Potential

It is convenient to obtain the solution in terms of a dimensionless system of variables. All lengths are nondimensionalized by dividing by the undisturbed jet width H , and the velocities are divided by $|V_\infty|$. The resulting configuration is shown in figure 2 in the first quadrant of the dimensionless physical plane.

As a result of the assumptions stated previously, the flow can be expressed in terms of a complex potential

$$W = \Phi + i\psi$$

where the potential function Φ and the stream function ψ are each governed by the Laplace equation. Since the derivative of Φ provides the local dimensionless velocity, and the curves of constant ψ are the streamlines, the solution of W within the jet will provide the complete flow field.

Boundary Conditions

In order to solve for W within the flow, Φ and ψ must be specified along the complete boundary of the flow. Along the axis of symmetry the velocity in the x direction must be zero. Also this line will arbitrarily be designated as the zero streamline. Then

$$\frac{\partial\Phi}{\partial x} = 0 \quad \psi = 0 \quad x = 0, y \geq 0 \quad (1)$$

Similarly along the x axis the y -velocity is zero and this axis is also part of the zero streamline

$$\frac{\partial\Phi}{\partial y} = 0 \quad \psi = 0 \quad y = 0, 0 \leq x \leq \infty \quad (2)$$

On the free streamlines the pressure is constant; since along these boundaries the jet is exposed to the external region that is at constant pressure. Consequently the velocity magnitude all along the free streamlines is equal to $|V_\infty|$, or $|v_\infty| = 1$. Hence, on the free streamlines

$$\left(\frac{\partial\Phi}{\partial x}\right)^2 + \left(\frac{\partial\Phi}{\partial y}\right)^2 = 1 \quad (3)$$

To determine the magnitudes of the stream functions on the free streamlines the Cauchy-Riemann equation

$$\frac{\partial \psi}{\partial x} = - \frac{\partial \Phi}{\partial y} = -v$$

is applied. Then between points 5 and 6 on figure 2

$$\psi - 0 = \int_6^5 -v \, dx = \int_6^5 -1 \, dx = -h_{5-6} = \psi_{4-5} \quad (4)$$

In a similar manner

$$\psi_{1-2} = +h_{1-9} \quad (5)$$

The asymptotic coordinates for the jet at its origin in figure 2 are

$$x_2 = s + \frac{h_{2-4}}{2} = s + \frac{1}{2} \quad y_2 = \infty \quad (6)$$

$$x_4 = s - \frac{h_{2-4}}{2} = s - \frac{1}{2} \quad y_4 = \infty \quad (7)$$

The amount of mass flow from each jet which is deflected toward the axis of symmetry, and toward the outside is not known a priori. As a result, the coordinates for points 1 and 5 cannot be completely specified in advance. Therefore, the remaining coordinates for the free streamlines are expressed implicitly as

$$x_5 = h_{5-6}(s) \quad y_5 = \infty \quad (8)$$

$$x_1 = \infty \quad y_1 = h_{1-9}(s) \quad (9)$$

The functions $h_{5-6}(s)$ and $h_{1-9}(s)$ as well as the shape of the free streamlines (the constant ψ_{4-5} and ψ_{1-2} lines) must be determined.

Conformal Mapping Method

The derivative of the potential W provides the complex conjugate of the vector velocity within the jet flow region.

$$\frac{dW}{dz} = u - iv = \zeta$$

By integrating, it is evident that the physical plane is related to the potential plane by means of an integration involving ζ

$$z = \int \zeta^{-1} dW + \text{constant} \quad (10)$$

The solution of equation (10) to determine the jet configuration in the z plane subject to the boundary conditions discussed in the previous section will be carried out by a technique whose development is generally attributed to Helmholtz and Kirchhoff (see ref. 1). As will be shown subsequently, the flow region in the W and ζ planes is known from available information. In order to integrate equation (10) these W and ζ regions are mapped conformally into an intermediate t plane. Once the $W(t)$ and $\zeta(t)$ transformation functions are known, they can be substituted into equation (10) and z as a function of t can be computed. Then the $z(t)$ function can be used to express $W(t)$ and $\zeta(t)$ implicitly in terms of z and thus solve the problem.

Hodograph ζ to auxiliary t plane transformation. - The hodograph ($\zeta = u - iv$) plane is shown in figure 3. The free streamlines (ψ_{1-2} and ψ_{4-5}) because of their property of having constant velocity magnitude are represented by the arcs 1-2 and 4-5 of the unit circle in the hodograph. The flow along the horizontal wall where $v = 0$ is represented by 7-a-8-9, while the axis of symmetry where $u = 0$ becomes the line 6-7 on the ζ plane. It should be noted that there are two stagnation points. Point 8 represents the coordinate about which each jet divides. Point 7 represents the stagnation point formed by the portions of each jet that impact at the origin of the z plane. In the z plane, point 8 may for some conditions fall on the axis of symmetry between 6 and 7 rather than lying on the real axis. This occurs when the spacing s is sufficiently small and will be discussed in detail in the section RESULTS AND DISCUSSION.

The domains representing the jet flow regions in the z and ζ planes are simply connected schlicht (sometimes referred to as simple) domains whose boundaries consist of more than one point. By Riemann's mapping theorem (ref. 3) these two domains are conformally equivalent and the conformal map $\zeta = \zeta(z)$ exists. Strictly speaking $\zeta(z)$ need be conformal only within the domain and not at every boundary point. Throughout this report we will follow the custom that the mapping will be referred to as conformal even though there are points on the boundary where this is not true.

Since the ζ domain has the properties described in the previous paragraph it in turn can be mapped conformally onto the simply-connected schlicht domain consisting of the interior of the unit semicircle in the auxiliary t -plane as shown in figure 4. The mapping is performed so that the free streamline arcs 1-2 and 4-5 transform to the half

circle with unit radius, and the straight line segments 6-7 and 7-8-9 go respectively into $-1 < t < 0$ and $0 < t < 1$ on the real axis. This is accomplished by the transformation (ref. 4)

$$\zeta = - \frac{t^{1/2}(t - A)}{At - 1} \quad \begin{array}{l} 0 \leq |t| \leq 1 \\ 0 \leq |A| \leq 1 \end{array} \quad (11)$$

where A corresponds to the distance in the t plane between the stagnation points 7 and 8. The points $t = 0$ and $t = A$ where $\zeta = 0$ represent the two stagnation points. This transformation has caused the straight lines which compose the multiple piece boundary 6-7-8-9 to become one straight line segment in the t plane.

The conjugate velocity ζ is now in terms of t , the variable in which equation (10) will eventually be integrated.

Complex potential W to auxiliary t plane transformation. - The complex potential $W = \Phi + i\psi$ must also be expressed in terms of t before the integration can be performed. The flow region in the W plane is shown in figure 5. The streamlines are parallel and the free streamlines form the upper and lower boundaries of the region at $\psi = h_{1-9}$ and h_{5-6} , respectively. The flow can be visualized as entering at the left and flowing toward the right between the free streamlines. The dotted streamline 3-8 is the line between the two portions the jet divides into as a result of the impact. The value of Φ at point 8 is arbitrarily taken as zero; this is permissible as will be shown.

The well-known Schwarz-Christoffel transformation (ref. 5) can be used to map a polygon onto the upper half plane. The flow region in the W plane can be considered a degenerate form of the dashed polygon, shown in figure 5. The points 5-6, 1-9, and 2-3-4 are formed by taking points c, d and e , respectively to infinity. In traveling around this polygon the change in exterior angle at each of points 9-1, 2-3-4, and 5-6 is $+\pi$ and the change at point 8 is $-\pi$ for a total change of 2π . Therefore, we use the degenerate Schwarz-Chrostoffel function

$$W(T) = \int \frac{B(T - T_8)dT}{(T - T_{1-9})(T - T_{2-3-4})(T - T_{5-6})} + F \quad (12)$$

to conformally map the interior of the region in the W plane onto the upper half T plane shown in figure 6. The polygon in the W plane is unfolded so that its entire boundary becomes the real axis in the T plane. Point 7 in the W plane is transformed to infinity in the T plane.

The final step of mapping the W plane into the t -plane is performed by the function

$$T = -\frac{1}{2} \left(t + \frac{1}{t} \right) \quad (13)$$

which conformally maps the upper half T plane into the unit semicircle shown in figure 4. Once the necessary constants are determined for the W mapping function in equation (12), $W(t)$ can be found by eliminating T by use of equation (13). Then $W(t)$ and $\zeta(t)$ from equation (11) can be substituted into the z equation (10) so it can be integrated.

Using partial fractions and simplifying the notation by letting T_{2-3-4} be T_3 , the integrand of equation (12) becomes (note that there are sufficient degrees of freedom in the transformation so that T_{1-9} and T_{5-6} have been fixed at -1 and $+1$, respectively):

$$\frac{T - T_8}{(T - T_{1-9})(T - T_{2-3-4})(T - T_{5-6})} = \frac{C}{T + 1} + \frac{D}{T - T_3} + \frac{E}{T - 1} \quad (14)$$

where

$$C = -\frac{1 + T_8}{2(1 + T_3)}$$

$$D = \frac{T_8 - T_2}{1 - T_3^2}$$

$$E = \frac{1 - T_8}{2(1 - T_3)}$$

The position T_8 can be found in terms of the parameter A which is the position of t_8 on figure 4. From equation (13)

$$T_8 = -\frac{1}{2} \left(A + \frac{1}{A} \right) \quad (15)$$

The quantity T_3 can also be found in terms of A . From equation (13)

$$T_3 = -\frac{1}{2} \left(t_3 + \frac{1}{t_3} \right) \quad (16a)$$

From equation (11) at point 3, $\zeta = i$ so that

$$i = - \frac{t_3^{1/2}(t_3 - A)}{At_3 - 1} \quad (16b)$$

If t_3 is eliminated from (16a) and (16b) the result is

$$T_3 = \frac{A^2 - 2A - 1}{2} \quad (17)$$

Equations (15) and (17) are substituted into C, D, and E to give

$$C = \frac{1}{2A} \quad (18a)$$

$$D = \frac{2}{A(A - 3)} \quad (18b)$$

$$E = - \frac{(A + 1)}{2A(A - 3)} \quad (18c)$$

Equation (14) is substituted into the integral of equation (12) and the integration is carried out to give

$$W = BC \ln(T + 1) + BD \ln(T - T_3) + BE \ln(T - 1) + K$$

The constant K is determined from the arbitrarily imposed condition $W = 0$ at $T = T_8$. This gives

$$W = BC \left[\ln(T + 1) - \ln(T_8 + 1) \right] + BD \left[\ln(T - T_3) - \ln(T_8 - T_3) \right] + BE \left[\ln(T - 1) - \ln(T_8 - 1) \right] \quad (19)$$

The coefficients will now be related to the jet widths h_{5-6} and h_{1-9} . To do this the imaginary part of W is utilized

$$\psi = BC \left[\arg(T + 1) - \arg(T_8 + 1) \right] + BD \left[\arg(T - T_3) - \arg(T_8 - T_3) \right] + BE \left[\arg(T - 1) - \arg(T_8 - 1) \right]$$

Since $T_8 + 1$, $T_8 - T_3$, and $T_8 - 1$ are all real and negative, this becomes

$$\psi = BC \left[\arg(T + 1) - \pi \right] + BD \left[\arg(T - T_3) - \pi \right] + BE \left[\arg(T - 1) - \pi \right] \quad (20)$$

In the region between T_{5-6} and T_7 , $\psi = 0$ and $T > 1 > T_3 > -1$. Hence

$$0 = BC(0 - \pi) + BD(0 - \pi) + BE(0 - \pi)$$

or

$$BC + BD + BE = 0 \quad (21a)$$

On the free streamline between points 4 and 5, equation (4) gives $\psi_{4-5} = -h_{5-6}$, and since $1 > T > T_3 > -1$,

$$-h_{5-6} = BC(0 - \pi) + BD(0 - \pi) + BE(\pi - \pi)$$

or

$$BC + BD = \frac{h_{5-6}}{\pi} \quad (21b)$$

On the free streamline between points 2 and 1, equation (5) gives $\psi_{2-1} = h_{1-9}$, and since $1 > T_3 > T > -1$

$$h_{1-9} = BC(0 - \pi) + BD(\pi - \pi) + BE(\pi - \pi)$$

or

$$BC = -\frac{h_{1-9}}{\pi} \quad (21c)$$

From continuity

$$h_{1-9} + h_{5-6} = 1 \quad (22)$$

Equations (21a), (21b), (21c), and (22) give

$$BC = -\frac{h_{1-9}}{\pi} \quad BD = \frac{1}{\pi} \quad \text{and} \quad BE = -\frac{h_{5-6}}{\pi} \quad (23)$$

From the relation $B = 1/\pi D$, B can be found by using D from equation (18b)

$$B = \frac{A(A - 3)}{2\pi} \quad (24)$$

Then

$$h_{1-9} = -\pi BC = \frac{1}{2} + \frac{1-A}{4} \quad (25a)$$

$$h_{5-6} = -\pi BE = \frac{1}{2} - \frac{1-A}{4} \quad (25b)$$

where C and E were used from equations (18a) and (18c).

Determination of $z(t)$. - With all coefficients of W related to the single parameter A, and the $\zeta(t)$ and $W(t)$ mapping functions available, the integration in the t plane can be performed. Equation (10) is written in the form

$$z - z_0 = \int_0^t \frac{1}{\zeta(t)} \frac{dW}{dT} \frac{dT}{dt} dt \quad (26)$$

Insert $\zeta(t)$ from equation (11), dW/dT from equation (12), and dT/dt from equation (13) to obtain

$$z - z_0 = \int_0^t \frac{At - 1}{t^{1/2}(t - A)} \frac{B(T - T_8)}{(T + 1)(T - T_3)(T - 1)} \frac{1}{2} \left(1 - \frac{1}{t^2}\right) dt$$

Now eliminate T by using equation (13), and T_8 and B by substituting their values in terms of A

$$z - z_0 = \int_0^t \frac{(At - 1) \left[\frac{A(A - 3)}{2\pi} \right] \left[-\frac{1}{2} \left(t + \frac{1}{t} \right) + \frac{1}{2} \left(A + \frac{1}{A} \right) \right] \left[\frac{1}{2} \left(1 - \frac{1}{t^2} \right) \right] dt}{\left[t^{1/2}(t - A) \right] \left[-\frac{1}{2} \left(t + \frac{1}{t} \right) + 1 \right] \left[-\frac{1}{2} \left(t + \frac{1}{t} \right) + \frac{1}{2} \left(t_3 + \frac{1}{t_3} \right) \right] \left[-\frac{1}{2} \left(t + \frac{1}{t} \right) - 1 \right]}$$

This can be simplified to

$$z - z_0 = \frac{A - 3}{\pi} \int_0^t \frac{(At - 1)^2 dt}{t^{1/2}(t + 1)(t - 1) \left(t - \frac{1}{t_3} \right) (t - t_3)} \quad (27)$$

The integration can be carried out by first expanding the integrand into partial fractions and then using the relation $(t_3 + 1/t_3) = 1 + 2A - A^2$ to give

$$z - z_0 = \frac{A - 1}{\pi} \left(\frac{1}{t_3 - 1} \right) \int_0^t \frac{dt}{t^{1/2} \left(t - \frac{1}{t_3} \right)} + \frac{1 - A}{\pi} \left(\frac{t_3}{t_3 - 1} \right) \int_0^t \frac{dt}{t^{1/2} (t - t_3)} \\ + \frac{A + 1}{2\pi} \int_0^t \frac{dt}{t^{1/2} (t + 1)} + \frac{A - 3}{2\pi} \int_0^t \frac{dt}{t^{1/2} (t - 1)} \quad (28)$$

The coordinate systems in figures 2 and 4 are such that $z = 0$ at $t = 0$. Hence, $z_0 = 0$. The integrals in equation (28) are then carried out to yield

$$z = \frac{1 - A}{\pi} \frac{t_3^{1/2}}{t_3 - 1} \ln \left(\frac{t_3^{-1/2} + t^{1/2}}{t_3^{-1/2} - t^{1/2}} \right) - \frac{1 - A}{\pi} \frac{t_3^{1/2}}{t_3 - 1} \ln \left(\frac{t_3^{1/2} + t^{1/2}}{t_3^{1/2} - t^{1/2}} \right) \\ + \frac{A + 1}{\pi} \tan^{-1} t^{1/2} + \frac{3 - A}{2\pi} \ln \frac{1 + t^{1/2}}{1 - t^{1/2}} \quad (29)$$

The parameter A in equation (29) will eventually be related to the dimensionless physical spacing s between the jets. The quantity t_3 can be related to A by using equations (16a) and (17). Since t_3 is on the unit semicircle in figure 4, it can be written as $e^{i\beta_3}$. Then

$$T_3 = -\frac{1}{2} \left(e^{i\beta_3} + e^{-i\beta_3} \right) = -\cos \beta_3$$

Using equation (17)

$$\beta_3 = \cos^{-1} \left(\frac{-A^2 + 2A + 1}{2} \right) \quad (30a)$$

Since

$$t_3 = \cos \beta_3 + i \sin \beta_3 \quad (30b)$$

the quantity t_3 can be found when A is assigned a value.

The general solution has now been obtained except for relating the quantity A to the actual physical spacing between the jets. This will be done when the equations are found for the free streamlines.

General Streamlines

The solution for the streamlines can be derived from equations (19) and (29). Beginning with equation (19) the relations for the coefficients in equations (18) and (24) are used to eliminate BC , BD , and BE in terms of A . Equation (13) is used to place T in terms of t , equation (15) is used for T_3 , and equation (17) for T_3 . After considerable manipulation, the imaginary part of W is taken to yield the stream function ψ

$$\psi = -\left(\frac{3-A}{2\pi}\right)\arg(t-1) - \left(\frac{A+1}{2\pi}\right)\arg(t+1) + \frac{\arg(t^2 + 2T_3t + 1)}{\pi}$$

which is equal to

$$\psi = \left(\frac{3-A}{2\pi}\right)\tan^{-1}\left(\frac{\eta}{1-\xi}\right) - \left(\frac{A+1}{2\pi}\right)\tan^{-1}\left(\frac{\eta}{1+\xi}\right) + \frac{1}{\pi}\tan^{-1}\left[\frac{\eta(2\xi + A^2 - 2A - 1)}{\xi^2 - \eta^2 + (A^2 - 2A - 1)\xi + 1}\right] \quad (31)$$

where

$$t = \xi + i\eta$$

Equation (29) for $z(t)$ can be separated into its real and imaginary parts to give

$$\begin{aligned}
x = & \left(\frac{3 - A}{4\pi} \right) \left[\ln \frac{1 + |t| + 2|t|^{1/2} \cos\left(\frac{\beta}{2}\right)}{1 + |t| - 2|t|^{1/2} \cos\left(\frac{\beta}{2}\right)} \right] + \left(\frac{A + 1}{2\pi} \right) \tan^{-1} \left[\frac{2|t|^{1/2} \cos\left(\frac{\beta}{2}\right)}{1 - |t|} \right] \\
& + \frac{\tan^{-1} \left(\frac{2|t|^{1/2} \sin \frac{\beta + \beta_3}{2}}{1 - |t|} \right)}{\pi} - \frac{\tan^{-1} \left(\frac{2|t|^{1/2} \sin \frac{\beta - \beta_3}{2}}{1 - |t|} \right)}{\pi} \quad (32)
\end{aligned}$$

$$\begin{aligned}
y = & \left(\frac{3 - A}{2\pi} \right) \left\{ \tan^{-1} \left[\frac{2|t|^{1/2} \sin\left(\frac{\beta}{2}\right)}{1 - |t|} \right] \right\} + \left(\frac{A + 1}{4\pi} \right) \left[\log \left(\frac{1 + |t| + 2|t|^{1/2} \sin \frac{\beta}{2}}{1 + |t| - 2|t|^{1/2} \sin \frac{\beta}{2}} \right) \right] \\
& + \frac{1}{2\pi} \log \left[\frac{\frac{1 + |t| + 2|t|^{1/2} \cos\left(\frac{\beta - \beta_3}{2}\right)}{1 + |t| - 2|t|^{1/2} \cos\left(\frac{\beta - \beta_3}{2}\right)}}{\frac{1 + |t| + 2|t|^{1/2} \cos\left(\frac{\beta + \beta_3}{2}\right)}{1 + |t| - 2|t|^{1/2} \cos\left(\frac{\beta + \beta_3}{2}\right)}} \right] \quad (33)
\end{aligned}$$

Equations (31) to (33) represent a set of parametric equations for determining ψ as a function of x and y . The $\psi = \text{constant}$ lines can be found by determining the ξ and η values from equation (31) for a specific ψ . Then these values of ξ and η are substituted into equations (32) and (33) to obtain the corresponding x and y coordinates.

Free Streamlines

Equations (32) and (33) become the equations for the free streamlines by substituting $|t| = 1$ which gives

$$x = \frac{3 - A}{4\pi} \left[\ln \left(\frac{1 + \cos \frac{\beta}{2}}{1 - \cos \frac{\beta}{2}} \right) \right] + \frac{A + 1}{4} \quad (34)$$

$$y = \frac{1}{2\pi} \ln \left[\frac{1 + \cos \left(\frac{\beta - \beta_3}{2} \right)}{1 - \cos \left(\frac{\beta - \beta_3}{2} \right)} \cdot \frac{1 + \cos \left(\frac{\beta + \beta_3}{2} \right)}{1 - \cos \left(\frac{\beta + \beta_3}{2} \right)} \right] + \frac{3 - A}{4} + \left(\frac{A + 1}{4\pi} \right) \left[\ln \left(\frac{1 + \sin \frac{\beta}{2}}{1 - \sin \frac{\beta}{2}} \right) \right] \quad (35)$$

for

$$\pi \geq \beta \geq \beta_3$$

and

$$x = \frac{3 - A}{4\pi} \left[\ln \left(\frac{1 + \cos \frac{\beta}{2}}{1 - \cos \frac{\beta}{2}} \right) \right] + \frac{A + 1}{4} + 1 \quad (36)$$

$$y = \frac{1}{2\pi} \ln \left[\frac{1 + \cos \left(\frac{\beta_3 - \beta}{2} \right)}{1 - \cos \left(\frac{\beta_3 - \beta}{2} \right)} \cdot \frac{1 + \cos \left(\frac{\beta_3 + \beta}{2} \right)}{1 - \cos \left(\frac{\beta_3 + \beta}{2} \right)} \right] + \frac{3 - A}{4} + \left(\frac{A + 1}{4\pi} \right) \left[\ln \left(\frac{1 + \sin \frac{\beta}{2}}{1 - \sin \frac{\beta}{2}} \right) \right] \quad (37)$$

for

$$\beta_3 \geq \beta \geq 0$$

Using the equation (7) boundary condition, equation (34) becomes

$$s = \frac{S}{H} = \frac{3 - A}{4\pi} \left[\ln \left(\frac{1 + \cos \frac{\beta_3}{2}}{1 - \cos \frac{\beta_3}{2}} \right) \right] + \frac{A + 3}{4} \quad (38)$$

This important equation gives the necessary link between the z and t planes by relating the parameter A in the t plane to the dimensionless half spacing (S/H). It is recalled that β_3 is related to A by equation (30a).

Pressure Distribution

When $\beta = 0$, t in figure 4 is a real positive number greater than or equal to zero and with a maximum value of 1. The corresponding points in the z plane lie on the real axis. Equation (11) for the velocity becomes

$$u = - \frac{\xi^{1/2}(\xi - A)}{\xi A - 1} \quad 0 \leq \xi \leq 1 \quad (39)$$

Incorporating this expression into Bernoulli's equation, the pressure coefficient becomes

$$C_p = \frac{p - p_a}{\frac{1}{2} \rho_j V_\infty^2} = 1 - u^2 = 1 - \frac{\xi(\xi - A)^2}{(\xi A - 1)^2} \quad 0 \leq \xi \leq 1 \quad (40)$$

For each ξ the corresponding position on the plate is from equation (32)

$$x = \frac{2}{\pi} \tan^{-1} \left[\frac{(1 - A)\xi^{1/2}}{1 - \xi} \right] + \frac{3 - A}{2\pi} \ln \left(\frac{1 + \xi^{1/2}}{1 - \xi^{1/2}} \right) + \frac{A + 1}{\pi} \tan^{-1} \xi^{1/2} \quad 0 \leq \xi \leq 1 \quad (41)$$

RESULTS AND DISCUSSION

As shown in the analysis, the configuration of the jet flow depends on only one parameter, the dimensionless half spacing (S/H) between the jets. The analytical solution came out more conveniently in terms of A which is related to S/H by means of equations (38) and (30a). The results will consist of a set of plots for various S/H of the free streamlines, the wall pressure coefficient, and some of the streamline patterns within the jets.

To compute the free streamlines, a value for A is first chosen. The quantity β_3 is then found from equation (30a) and the jet spacing is found from equation (38). Equations (34) to (37) can then be used to compute the free streamlines. The pressure coefficient is found by letting ξ vary between 0 and 1 in equations (40) and (41). This gives C_p and the corresponding x values along the wall.

The streamline pattern within the jets is computed from equations (31) to (33). An arbitrary pair of ξ and η values are chosen which correspond to a point within the unit semicircle of figure 4 (i. e., $|t| = \sqrt{\xi^2 + \eta^2} < 1$). The value of the stream function is then computed from equation (31). The physical coordinates x and y corresponding to this value of ψ are then found from equations (32) and (33). By doing this for numerous $|t|$ points within the unit semicircle, the entire streamline pattern can be mapped.

Figure 7 shows the results for several jet spacings corresponding to positive values of A . For positive A the stagnation point 8 lies on the x axis as shown in figure 2. Figure 7(a) shows the configuration for a large spacing between jets; in this case the spacing between the two jets is about 6 jet widths (half-spacing $S/H = 3.132$). Each jet acts practically independently and divides so that half of the flow goes toward $x = +\infty$ and half toward $x = 0$ where the portions of the two jets merge to form a jet one width wide moving toward $y = +\infty$. The incident fluid stream is not influenced by the plate until it is within about two jet widths from the plate.

The pressure coefficient in figure 7(a) is unity at the two stagnation points where there is complete recovery of the velocity energy for the inviscid conditions considered here. At $X/H = 5$, $C_p \approx 0$, indicating that the flow has completely turned and the velocity magnitude along the wall is $|V_\infty|$.

The other three parts of figure 7 show similar jet patterns as the jet spacing is decreased which causes the stagnation point 8 to move closer to the stagnation point 7. Figure 7(d) shows a typical streamline pattern, and in this instance in the region of $X/H = 0.8$ the C_p decreases only a small amount from unity. This shows that the region near the wall between the two stagnation points is essentially a stagnation region. The low velocity in this region is evidenced by the wide spacing between the streamlines $\psi = -0.1$ and $\psi = 0$.

Figure 8 shows the flow configuration when $A = 0$ which causes all the stagnation

points to coincide at the origin. This corresponds to a half spacing of 1.379 jet widths.

A further decrease in jet spacing below that of figure 8 produces the series of flow patterns in figure 9. Here the dividing streamline $\psi = 0$ ends at a stagnation point along the y axis of symmetry. Part of the jet is turned and moves back toward $y = +\infty$ without penetrating very close to the wall. As the spacing is further decreased the stream flowing back along the y -axis is diminished in width and is formed further away from the wall. In figure 9(c) there is practically no backward circulation and the two jets have almost merged to form a single jet of width $2H$ centered about the y -axis.

The percent of recirculation up the y -axis, as a function of dimensionless half spacing (S/H), can be determined from equations (25b), (30a), and (38). A plot of the percentage recirculation $100 h_{5-6}$ as a function of S/H is shown in figure 10. Note that when $S/H = 0.5$, the two jets have merged into a single one and there is no recirculating flow.

CONCLUDING REMARKS

Conformal mapping has been applied to determine the flow pattern and pressure coefficient resulting from two parallel inviscid slot jets impinging normally on a surface. After being turned by the surface a portion of each jet flows outward in a region where the flow becomes parallel to the plate. The remainder of the flow turns inward toward the axis of symmetry between the jets; these portions of the two jets collide and a recirculation occurs back between the two incoming jets.

The extent of the recirculation region depends on a single parameter which is the spacing in jet widths between the centerlines of the incident jets. For a spacing greater than about 6 jet widths, one-half of each jet recirculates. For a spacing less than 2 jet widths the recirculation is less than 10 percent. The spacing also determines the type of flow pattern. When the spacing is larger than about 2.8 jet widths, there are three stagnation points on the plate, one under each impinging jet and one at the axis of symmetry. For a spacing of 2.8 jet widths there is only one stagnation point; it is on the plate at the line of symmetry. For a smaller spacing there are two stagnation points along the line of symmetry; one of them on the plate and the other within the flow.

Probably the most frequently occurring practical situation which best fits these results is two liquid jets impinging on a vertical wall in the presence of a gaseous atmosphere. As indicated by the results, the incoming flow a few jet widths away from the impact region is essentially uniform and of velocity magnitude $|V_\infty|$. The fact that the jets do not originate at infinity or that the return flow does not reach infinity is not very significant. For this cited jet case to apply we require only that the jets originate with a uniform velocity at a distance about $2H$ to $4H$ away from the plate.

The pressure distribution along the plate for the cited liquid jet in air is of practical value. Portions of the pressure distribution can be used for calculating the boundary layer and heat transfer between the plate and jet. In the case where $1 < S/H < 2.5$, the pressure coefficient should be valid from $X/H = 0$ to $X/H \cong 4$. Beyond $X/H \cong 4$, the entrainment effects and wall boundary layer become significant and the flow approaches a viscous wall jet. As the jet spacing is increased beyond 2.5; the entrainment effects on the recirculating portion of the jet, at small X/H , will significantly affect the C_p , invalidating the inviscid analysis in the region of the stagnation point (point 7) at $X = 0$.

When the jet and surrounding fluid are the same, entrainment effects can invalidate the C_p solution throughout the stagnation zone regions. The incoming jet interacts with the recirculating portion to retard the incoming jet flow. As a result the C_p will be less than 1 at the stagnation points. This has been experimentally shown in reference 6.

The analytical techniques used to solve the current jet flow can be used for the solution of any problem governed by Laplace's equation with boundaries consisting of straight surfaces and free streamlines. For instance, the solidification of a flowing liquid on a cold surface has recently been analyzed in reference 7 using these techniques.

Lewis Research Center,
National Aeronautics and Space Administration
Cleveland, Ohio, September 25, 1968,
129-01-07-07-22.

REFERENCES

1. Milne-Thomson, L. M.: Theoretical Hydrodynamics. The Macmillan Co., 1938.
2. Gardon, Robert; and Akfirat, J. Cahit: The Role of Turbulence in Determining the Heat-Transfer Characteristics of Impinging Jets. Int. J. Heat Mass Transfer, vol. 8, Oct. 1965, pp. 1261-1272.
3. Nehari, Zeev: Conformal Mapping. McGraw-Hill Book Co., Inc., 1952.
4. Birkhoff, Garrett; and Zarantonello, E. H.: Jets, Wakes, and Cavities. Academic Press, Inc., 1957.
5. Churchill, Ruel V.: Complex Variables and Applications. Second ed., McGraw-Hill Book Co., Inc., 1960.
6. Gardon, Robert; and Akfirat, J. Cahit: Heat Transfer Characteristics of Impinging Two-Dimensional Air Jets. J. Heat Transfer, vol. 88, no. 1, Feb. 1966, pp. 101-108.

7. Siegel, Robert: Conformal Mapping for Steady Two-Dimensional Solidification on a Cold Surface in Flowing Liquid. NASA TN D-4771, 1968.

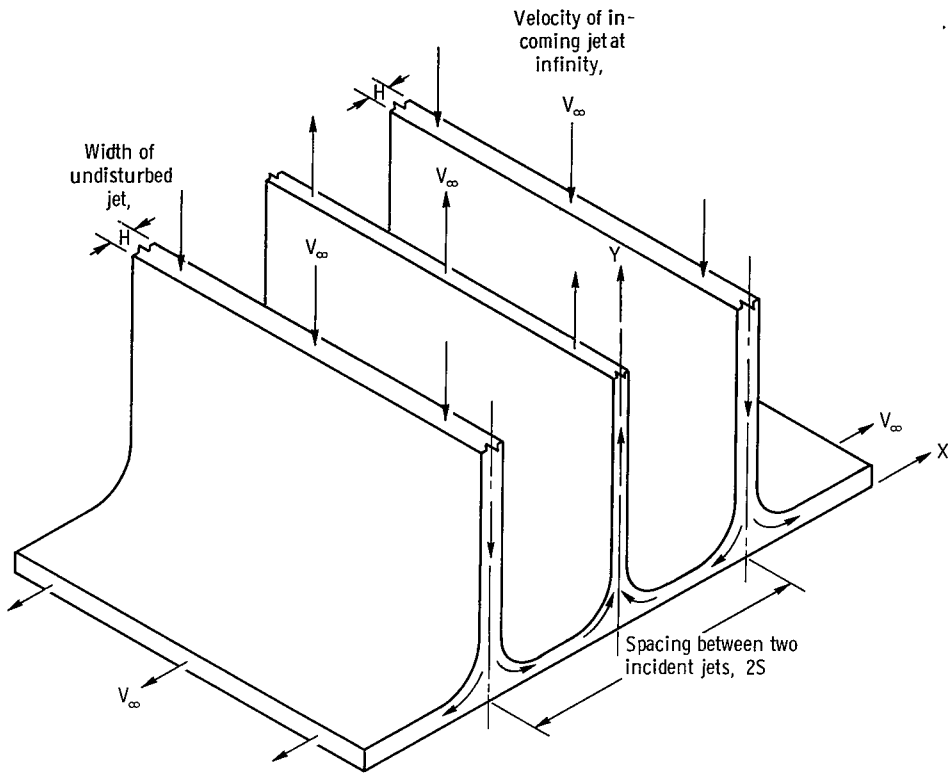


Figure 1. - Impingement of two parallel jets on horizontal plane.

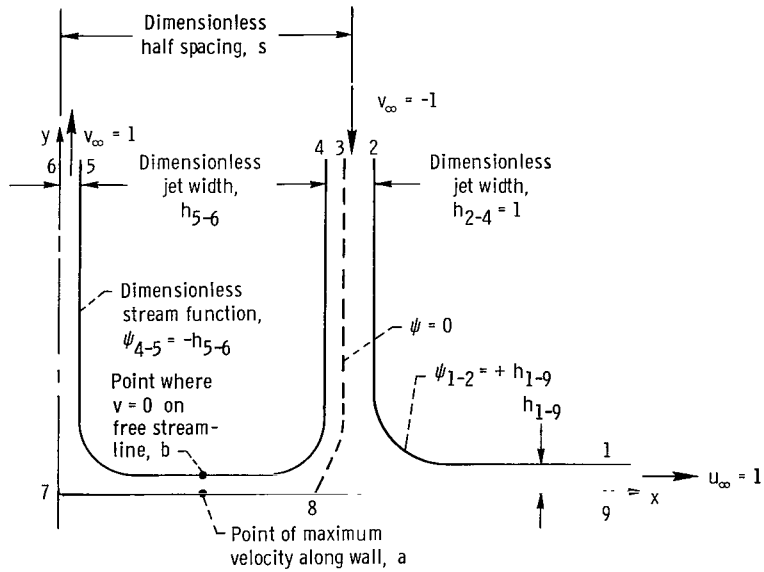


Figure 2. - Jet flow in first quadrant of dimensionless z-plane.

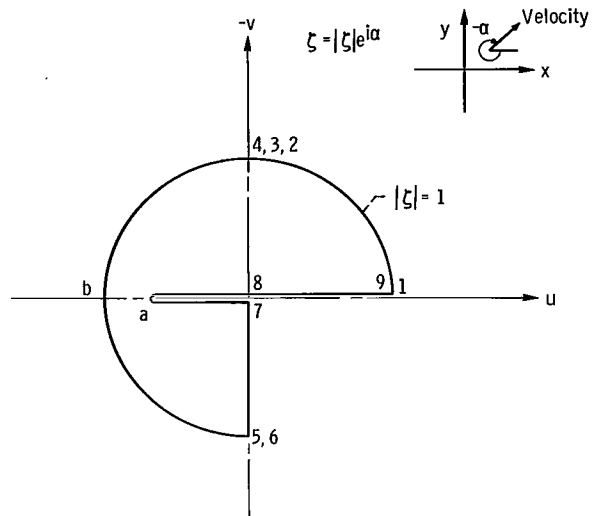


Figure 3. - Hodograph plane $\zeta = u - iv$.

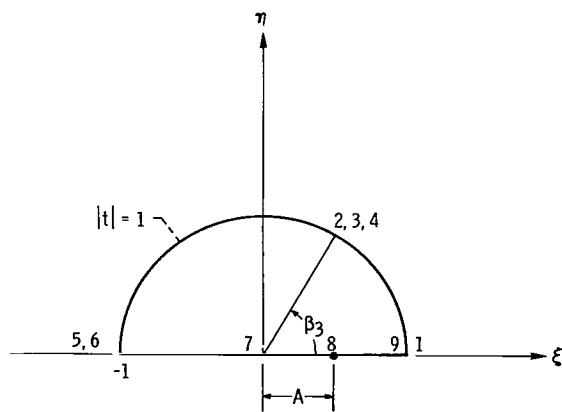


Figure 4. - Auxiliary t -plane, $t = \xi + i\eta = |t|e^{i\beta}$.

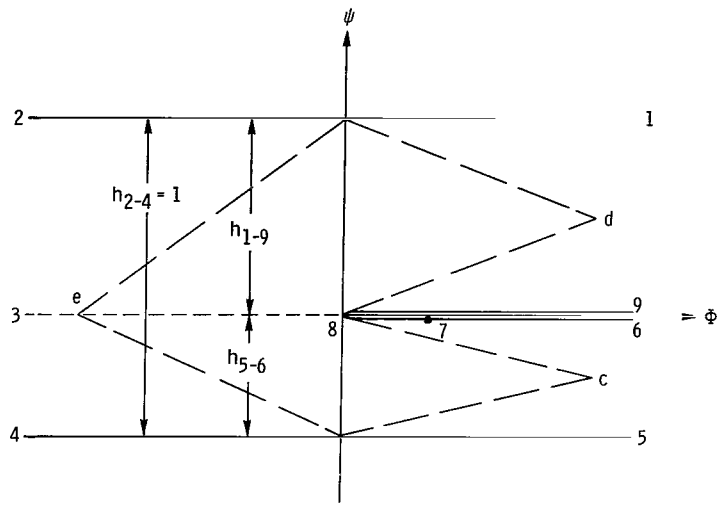


Figure 5. - Potential plane $W = \Phi + i\psi$.

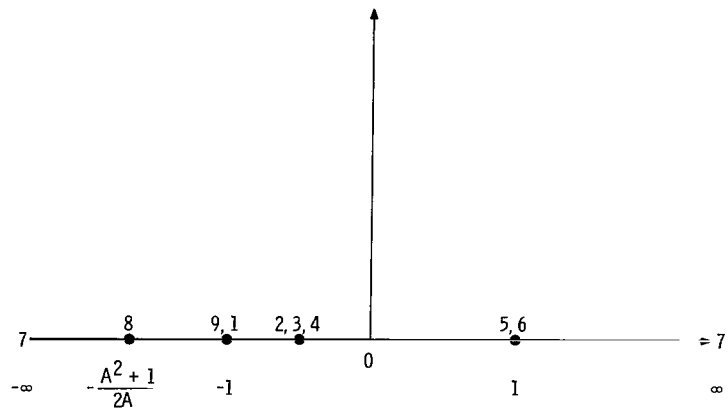
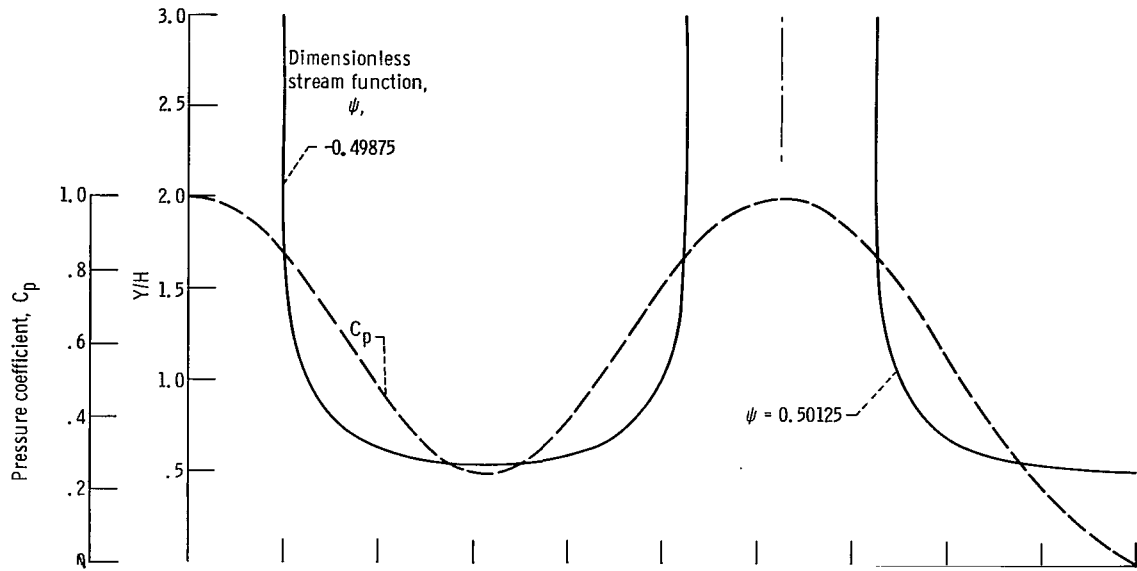
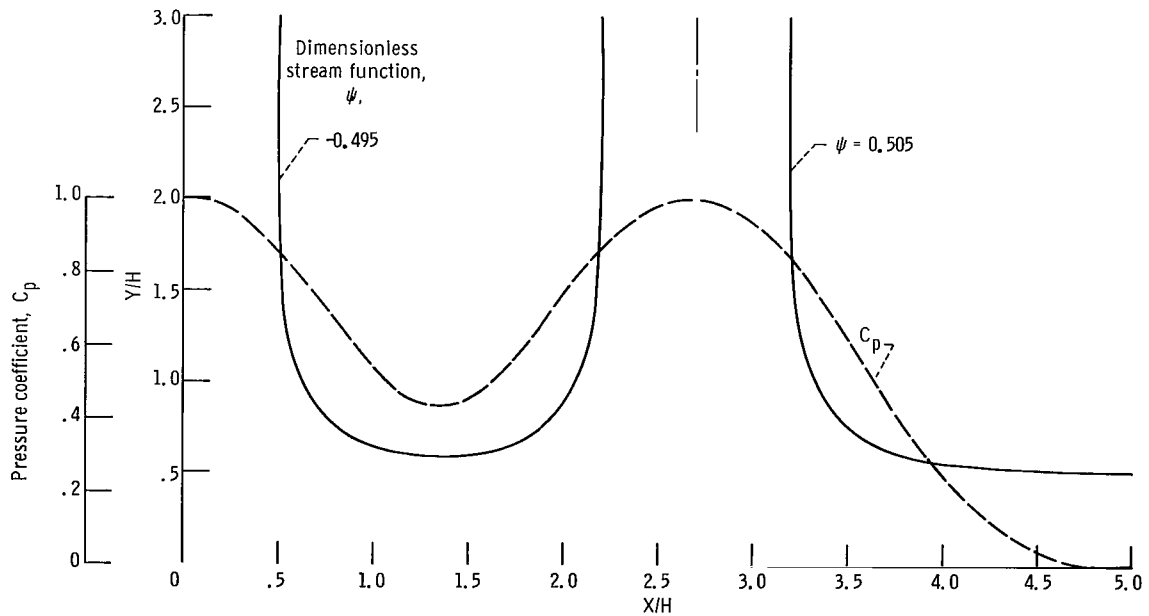


Figure 6. - Auxiliary T-plane.

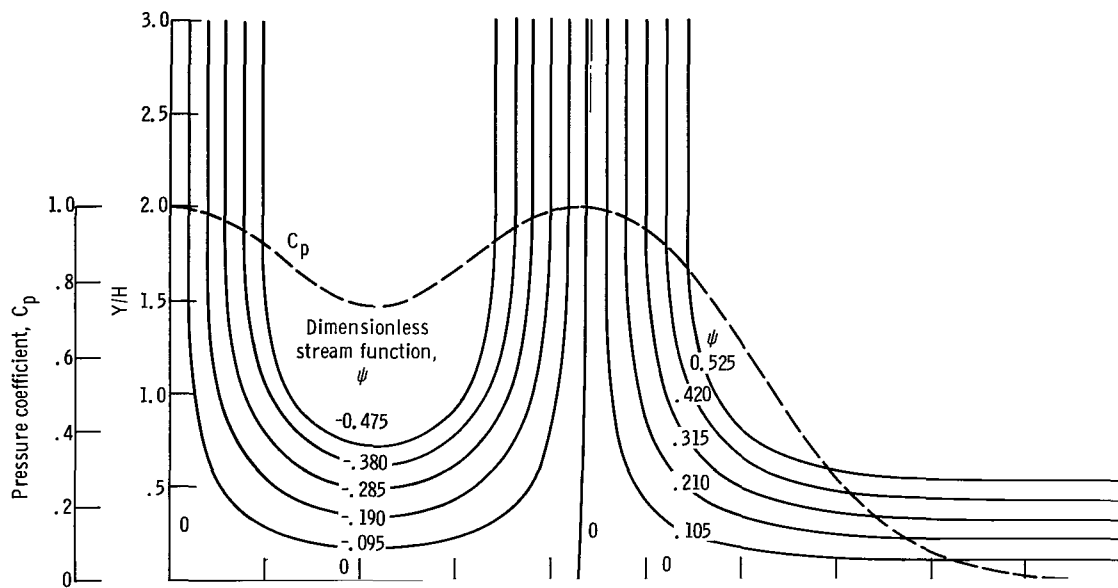


(a) Ratio of half spacing between jets to jet width, $S/H = 3.132$ ($A = 0.995$).

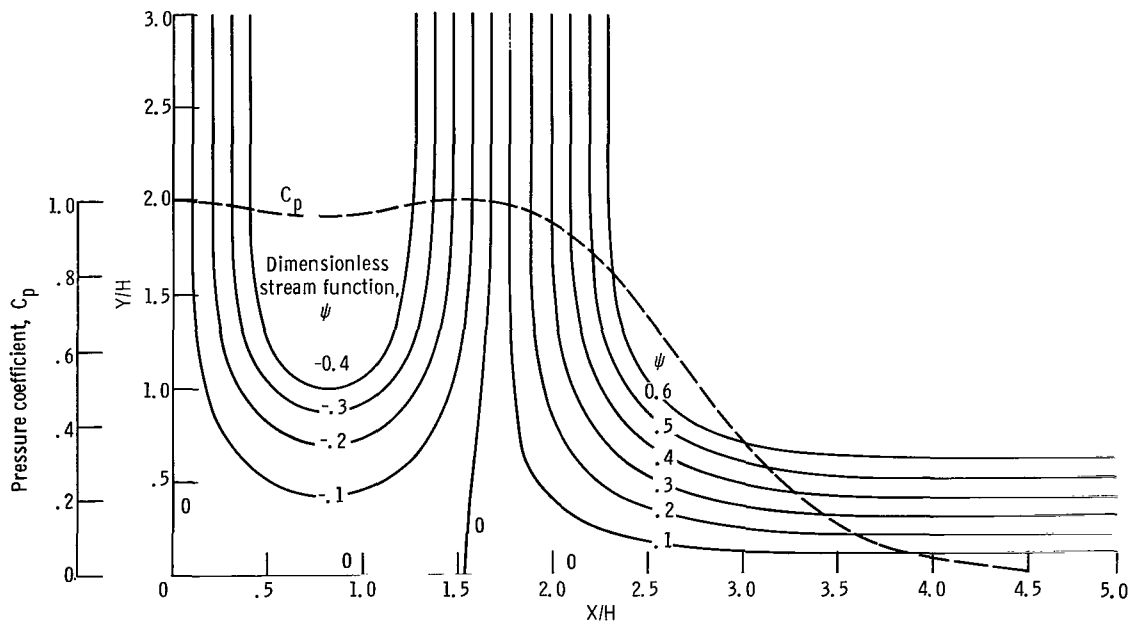


(b) Ratio of half spacing between jets to jet width, $S/H = 2.698$ ($A = 0.98$).

Figure 7. - Jet configurations for sufficiently large spacings so that all stagnation points are on wall.



(c) Ratio of half spacing between jets to jet width, $S/H = 2.208$ ($A = 0.9$).



(d) Ratio of half spacing between jets to jet width, $S/H = 1.775$ ($A = 0.6$).

Figure 7. - Concluded.

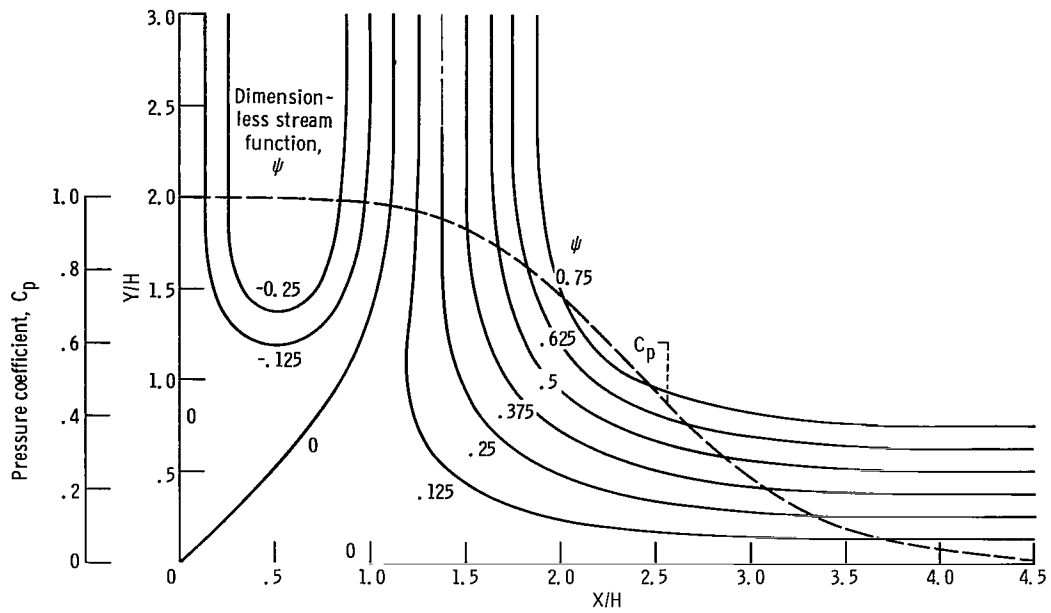
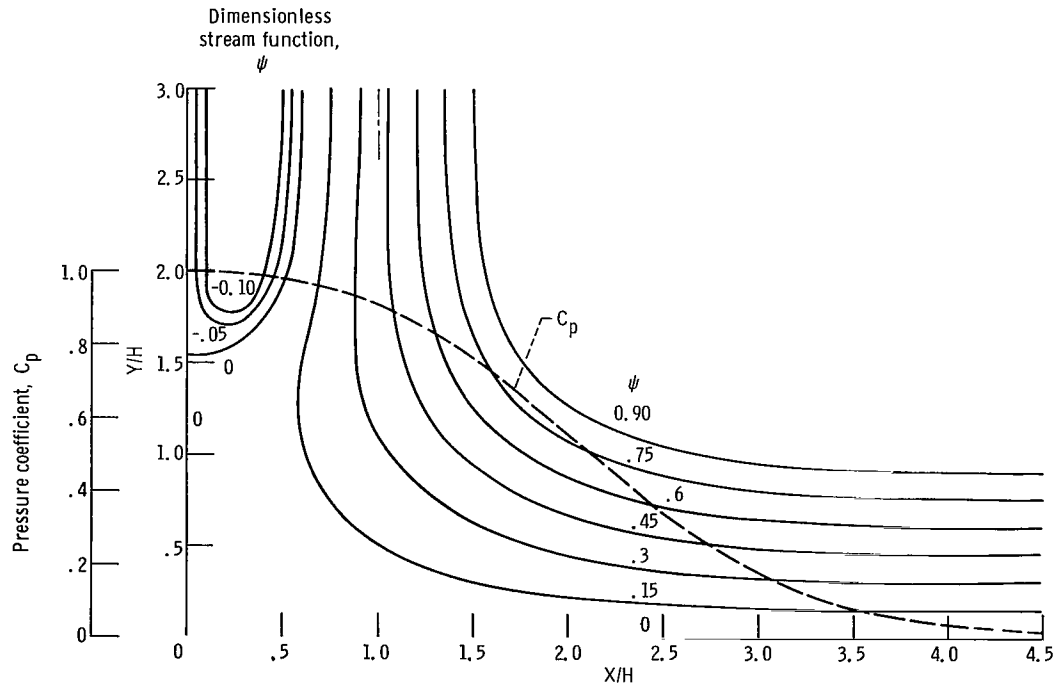
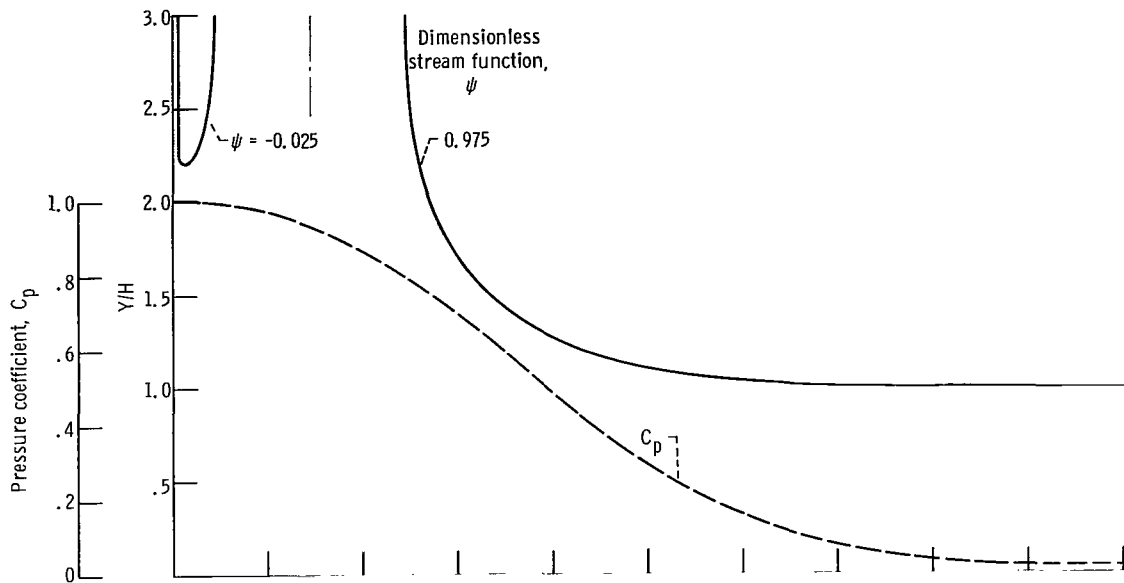


Figure 8. - Jet configuration when all stagnation points coincide. Ratio of half spacing between jets to jet width, $S/H = 1.379$ ($A = 0$).

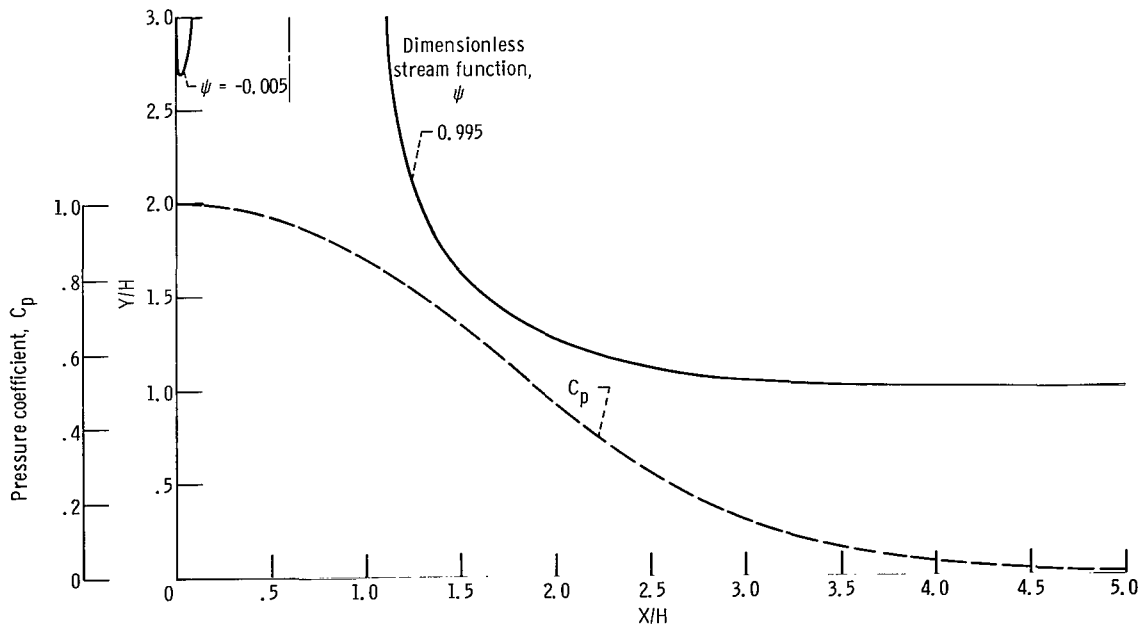


(a) Ratio of half spacing between jets to jet width, $S/H = 0.997$ ($A = -0.6$).

Figure 9. - Jet configuration when jet spacing is sufficiently small so that there is a stagnation point on the line of symmetry.



(b) Ratio of half spacing between jets to jet width, $S/H = 0.725$ ($A = -0.9$).



(c) Ratio of half spacing between jets to jet width, $S/H = 0.595$ ($A = -0.98$).

Figure 9. - Concluded.

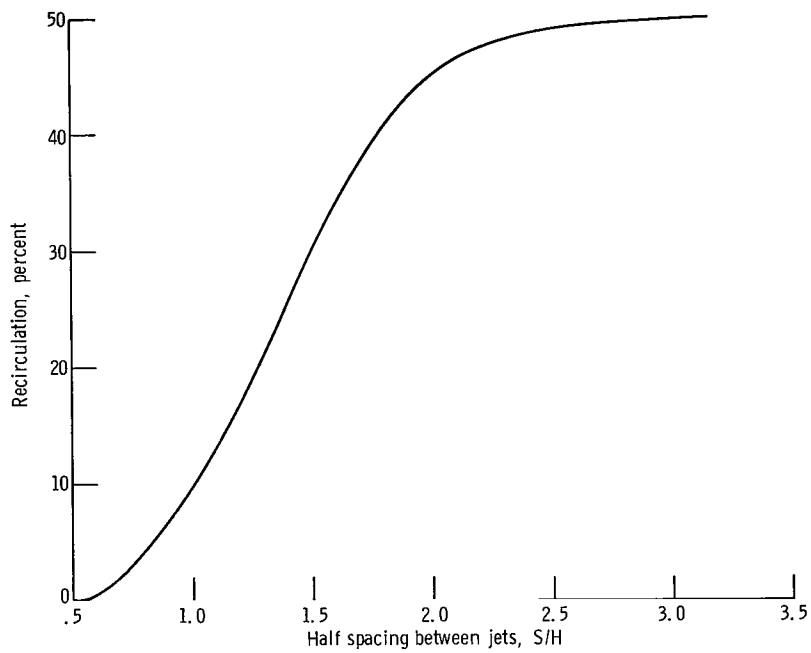


Figure 10. - Percent of flow recirculating back along Y-axis as function of half spacing between jets.

POSTMASTER: If Undeliverable (Section 158
Postal Manual) Do Not Return

"The aeronautical and space activities of the United States shall be conducted so as to contribute . . . to the expansion of human knowledge of phenomena in the atmosphere and space. The Administration shall provide for the widest practicable and appropriate dissemination of information concerning its activities and the results thereof."

— NATIONAL AERONAUTICS AND SPACE ACT OF 1958

NASA SCIENTIFIC AND TECHNICAL PUBLICATIONS

TECHNICAL REPORTS: Scientific and technical information considered important, complete, and a lasting contribution to existing knowledge.

TECHNICAL NOTES: Information less broad in scope but nevertheless of importance as a contribution to existing knowledge.

TECHNICAL MEMORANDUMS: Information receiving limited distribution because of preliminary data, security classification, or other reasons.

CONTRACTOR REPORTS: Scientific and technical information generated under a NASA contract or grant and considered an important contribution to existing knowledge.

TECHNICAL TRANSLATIONS: Information published in a foreign language considered to merit NASA distribution in English.

SPECIAL PUBLICATIONS: Information derived from or of value to NASA activities. Publications include conference proceedings, monographs, data compilations, handbooks, sourcebooks, and special bibliographies.

TECHNOLOGY UTILIZATION PUBLICATIONS: Information on technology used by NASA that may be of particular interest in commercial and other non-aerospace applications. Publications include Tech Briefs, Technology Utilization Reports and Notes, and Technology Surveys.

Details on the availability of these publications may be obtained from:

**SCIENTIFIC AND TECHNICAL INFORMATION DIVISION
NATIONAL AERONAUTICS AND SPACE ADMINISTRATION
Washington, D.C. 20546**